

Synthesis and properties of mixed-metal phosphido and phosphinidene clusters derived from reaction between $\text{Ru}_3(\text{CO})_{10}(\mu\text{-H})(\mu\text{-PPh}_2)$ and $\text{Cp}^*\text{Mo}(\text{CO})_3\text{H}$

Jar-Chen Wang^a, Yun Chi^a, Shie-Ming Peng^b, Gene-Hsiang Lee^b, Shin-Guang Shyu^c and Fung-Huang Tu^a

^a Department of Chemistry, National Tsing Hua University, Hsinchu 30043 (China)

^b National Taiwan University, Taipei 10764 (Taiwan)

^c Institute of Chemistry, Academia Sinica, Taipei 11529 (Taiwan)

(Received October 27, 1993)

Abstract

The tetranuclear phosphido cluster $\text{Cp}^*\text{MoRu}_3(\text{CO})_{10}(\mu\text{-H})_2(\mu\text{-PPh}_2)$ (**5**) and the phosphinidene cluster $\text{Cp}^*\text{MoRu}_3(\text{CO})_{10}(\mu_3\text{-H})(\mu_3\text{-PPh})$ (**6**) have been synthesized by reaction of $\text{Ru}_3(\text{CO})_{10}(\mu\text{-H})(\mu\text{-PPh}_2)$ with excess molybdenum hydride $\text{Cp}^*\text{Mo}(\text{CO})_3\text{H}$ in refluxing toluene solution. Crystals of **5** are monoclinic, space group $P 2_1$, with $a = 10.708(2)$, $b = 10.848(4)$, $c = 14.885(2)$ Å, $\beta = 97.63(2)^\circ$, $Z = 2$, $R = 0.021$, $R_w = 0.019$ for 3025 observed reflections. The cluster has a tetrahedral array of metal atoms with one edge-bridging and one face-bridging hydride, and a phosphido ligand bridged across a basal Ru–Ru edge. Thermolysis of **5** under similar conditions produced the phosphinidene cluster **6** in high yield via elimination of a benzene molecule, indicating that **5** is an intermediate in the formation of **6**. Subsequent treatment of **6** with CO caused fragmentation of the cluster affording a trinuclear phosphinidene cluster $\text{Cp}^*\text{MoRu}_2(\text{CO})_8(\mu\text{-H})(\mu_3\text{-PPh})$ (**7**). Dimerization of **7** occurred upon thermolysis to afford hexanuclear $\text{Cp}_2^*\text{Mo}_2\text{Ru}_4(\text{CO})_{12}(\mu\text{-PPh})_2$ (**8**), which has also been characterized by X-ray diffraction. Crystal data of **8**: space group $C 2/c$; $a = 45.333(7)$, $b = 10.185(2)$, $c = 21.915(8)$ Å, $\beta = 93.82(3)^\circ$, $Z = 8$. The structure was solved by direct method and refined to R and R_w of 0.035 and 0.030 for 6135 observed reflections with $I > 2\sigma(I)$. The molecule adopts a square pyramidal MoRu_4 skeleton with a tentacle Mo atom bridging a Ru–Ru edge, on which the novel $\mu_4\text{-}\eta^2\text{-CO}$ ligand is associated with the butterfly Mo_2Ru_2 array; one $\mu_4\text{-PPh}$ ligand occupies a MoRu_3 square face and a second $\mu_3\text{-PPh}$ ligand caps a MoRu_2 face.

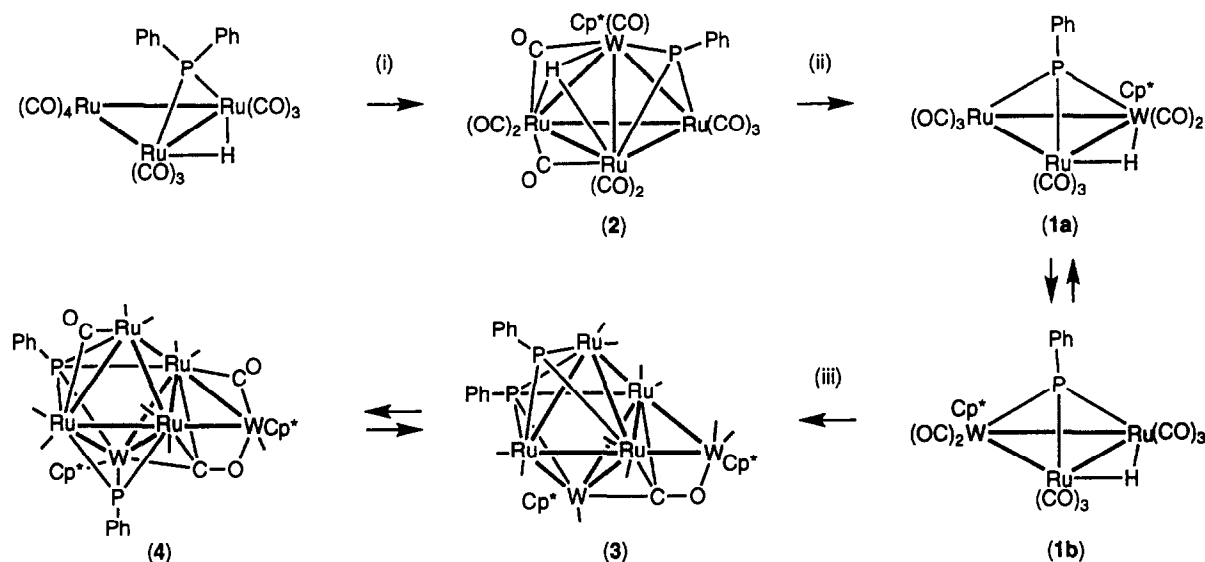
Key words: Ruthenium; Molybdenum; Phosphido; Phosphinidene

1. Introduction

The chemistry of mixed-metal clusters of transition-metals has been the subject of considerable research activity [1]. This has been stimulated by a belief that the various metals present in mixed-metal clusters may show reactivity patterns or structure very different from those of their homometallic analogues. With the aims of examining and comparing the basic of patterns of reactivity of heterometallic clusters, we have synthesized and characterized a series of trimetallic imido clusters $\text{LWRu}_2(\text{CO})_8(\mu\text{-H})(\mu_3\text{-NPh})$, $\text{L} = \text{Cp}$ and Cp^* [2], and closely related phosphinidene clusters

$\text{LWRu}_2(\text{CO})_8(\mu\text{-H})(\mu_3\text{-PPh})$ (**1a**, $\text{L} = \text{Cp}$, **1b**, $\text{L} = \text{Cp}^*$) [3]. The reactivities of these imido and phosphinidene heterometallic clusters have been explored [4]. In contrast to the higher thermal stability of imido clusters, the phosphinidene derivative **1b**, which was obtained from the direct treatment of $\text{Ru}_3(\text{CO})_{10}(\mu\text{-H})(\mu\text{-PPh}_2)$ with $\text{Cp}^*\text{W}(\text{CO})_3\text{H}$ through the formation of a tetranuclear precursor $\text{Cp}^*\text{WRu}_3(\text{CO})_{10}(\mu_3\text{-H})(\mu_3\text{-PPh})$ (**2**), can undergo dimerization by elimination of H_2 and CO to afford two hexanuclear cluster derivatives (**3**) and (**4**) with an identical structural formula $\text{Cp}_2^*\text{W}_2\text{Ru}_4(\text{CO})_{12}(\mu\text{-PPh})_2$ (Scheme 1) [5]. This variation in reactivity regarding the phosphinidene clusters is clearly due to the phosphorus atom being bigger than nitrogen, and the possibility of increased coordination capability [6].

Correspondence to: Dr. Y. Chi



Scheme 1.

In the present work on cluster assembly reactions, we have varied the transition-metal atoms in an attempt to examine the influence of transition metal atoms on the structure and reactivity of cluster compounds. We therefore reacted $\text{Ru}_3(\text{CO})_{10}(\mu\text{-H})(\mu\text{-PPh}_2)$ with $\text{Cp}^*\text{Mo}(\text{CO})_3\text{H}$. From the reaction mixture, a small amount of an unknown phosphido cluster $\text{Cp}^*\text{MoRu}_3(\text{CO})_{10}(\mu\text{-H})_2(\mu\text{-PPh}_2)$ (5) was isolated, in addition to the expected tetranuclear phosphinidene cluster $\text{Cp}^*\text{MoRu}_3(\text{CO})_{10}(\mu_3\text{-H})(\mu_3\text{-PPh})$ (6) and trinuclear cluster $\text{Cp}^*\text{MoRu}_2(\text{CO})_8(\mu\text{-H})(\mu_3\text{-PPh})$ (7); their relationships were established. Furthermore, heating of 7 in toluene afforded only one hexanuclear derivative $\text{Cp}_2^*\text{Mo}_2\text{Ru}_4(\text{CO})_{12}(\mu\text{-PPh})_2$ (8), which is isostructural with 4 but not with 3, as indicated by X-ray diffraction measurements. In connection with the tungsten-ruthenium and molybdenum-ruthenium phosphinidene clusters that we synthesized, Schauer and Carty have described the preparation of both a triruthenium phosphinidene cluster $[\text{Ru}_3(\text{CO})_9(\mu\text{-H})(\mu_3\text{-PPh})]^-$ by deprotonation of $\text{Ru}_3(\text{CO})_{10}(\mu\text{-H})(\mu\text{-PPh})$ [7] and a novel nickel-ruthenium cluster $\text{Cp}_2\text{Ni}_2\text{Ru}_3(\text{CO})_9(\mu_5\text{-PPh})$ via condensation of unsaturated trinuclear cluster $\text{Ru}_3(\text{CO})_9(\mu\text{-H})(\mu\text{-PPh}_2)$ with $[\text{CpNi}(\text{CO})_2]$ [8], respectively.

2. Experimental procedure

2.1. General information and materials

Infrared spectra were recorded on a Perkin-Elmer 2000 FT-IR spectrometer. ^1H and ^{13}C NMR spectra were recorded on a Bruker AM-400 and a Varian Unity-400 instrument, whereas ^{31}P NMR spectra were recorded on a Bruker AMX-300 instrument. Chemical

shifts are quoted with respect to internal standard tetramethylsilane (^1H and ^{13}C NMR) and external standard 85% H_3PO_4 (^{31}P NMR). Mass spectra were obtained on JEOL-HX110 instrument operating in fast atom bombardment (FAB) mode. The phosphido bridged triruthenium complex $\text{Ru}_3(\text{CO})_{10}(\mu\text{-H})(\mu\text{-PPh}_2)$ was prepared from the reaction of $\text{Ru}_3(\text{CO})_{12}$ with diphenylphosphine in THF with sodium benzophenone ketyl as catalyst followed by thermolysis at 50 to 55°C in heptane solution [9]. Molybdenum hydride complex $\text{Cp}^*\text{Mo}(\text{CO})_3\text{H}$ was prepared from reaction of (*para*-xylene) $\text{Mo}(\text{CO})_3$ with pentamethylcyclopentadiene [10]. All reactions were performed under a nitrogen atmosphere using deoxygenated solvents dried with an appropriate reagent. The progress of reactions was monitored by analytical thin-layer chromatography (5735 Kieselgel 60 F₂₅₄, E. Merck) and the products were separated on thin-layer chromatographic plates (Kieselgel 60 F₂₅₄, E. Merck). Elemental analyses were performed at the NSC Regional Instrumentation Center at National Cheng Kung University, Tainan, Taiwan.

2.2. Reaction of $\text{Ru}_3(\text{CO})_{10}(\mu\text{-H})(\mu\text{-PPh}_2)$ with $\text{Cp}^*\text{Mo}(\text{CO})_3\text{H}$

In a 100 ml round bottom reaction flask, the phosphido complex $\text{Ru}_3(\text{CO})_{10}(\mu\text{-H})(\mu\text{-PPh}_2)$ (100 mg, 0.128 mmol) and molybdenum hydride $\text{Cp}^*\text{Mo}(\text{CO})_3\text{H}$ (160 mg, 0.40 mmol) were dissolved in a toluene solution (50 ml) and kept at reflux for 20 min. The colour changed gradually from orange to dark brown. After the solution was cooled to room temperature, the solvent was evaporated *in vacuo* and the residue was separated by thin layer chromatography (dichloro-

TABLE 1. Experimental data for the X-ray diffraction studies of complexes 5 and 8

Compound	5	8
Formula	C ₃₂ H ₂₅ O ₁₀ P ₁ Mo ₁ Ru ₃	C ₄₅ H ₄₂ Cl ₂ O ₁₂ P ₂ Mo ₂ Ru ₄
Mol. wt.	999.66	1503.83
Crystal system	Monoclinic	Monoclinic
Space group	P2 ₁	C2/c
a (Å)	10.708(2)	45.333(7)
b (Å)	10.848(4)	10.185(2)
c (Å)	14.885(2)	21.915(8)
β (°)	97.63(2)	93.82(3)
U (Å ³)	1713.8(8)	10 096(4)
Temperature	25°C	25°C
Z	2	8
D _c (g cm ⁻³)	1.937	1.979
F(000)	972	5856
Crystal size, mm.	0.20 × 0.45 × 0.45	0.25 × 0.50 × 0.50
h, k, l ranges	-12 12, 0 12, 0 17	-51 51, 0 11, 0 24
μ (mm ⁻¹)	1.68	1.84
Absorption (T _{min} & T _{max})	0.80, 1.00	0.93, 1.00
No. of unique data (2θ _{max})	3180 (50)	7898 (48)
data with I > 2σ(I)	3025	6135
No. of atoms	72	109
No. of variables	432	577
R; R _w	0.021; 0.019	0.035; 0.030
G.O.F.	2.09	2.22

methane: hexane = 1 : 7), giving 13 mg of red Ru₄(CO)₁₃(μ₃-PPh) (0.015 mmol, 12%), 10 mg of green Ru₅(CO)₁₅(μ₄-PPh) (0.01 mmol, 7%), 47 mg of orange Cp*MoRu₂(CO)₈(μ-H)(μ₃-PPh) (7, 0.063 mmol, 42%), 6 mg of black phosphido cluster Cp*MoRu₃(CO)₁₀(μ-H)₂(μ-PPh₂) (5, 0.006 mmol, 4.7%) and 15 mg of dark-red cluster Cp*MoRu₃(CO)₁₀(μ₃-H)(μ₃-PPh) (6, 0.016 mmol, 13%) in the order of their elution.

Spectral data of 5: MS (FAB, ⁹⁸Mo, ¹⁰²Ru), *m/z* 1006 (M⁺); IR (C₆H₁₂) ν(CO): 2072s, 2021vs, 2006vw, 1997m, 1974s, 1865w, br, 1805w, br cm⁻¹; ¹H NMR (CD₂Cl₂, RT): δ 7.91–6.96 (m, 10H), 1.98 (s, 15H), -13.65 (d, J_{P-H} = 19.6 Hz), -19.52 (d, J_{P-H} = 11.2 Hz). ¹³C NMR (CD₂Cl₂, RT): CO, δ 242.5 (d, 2C, J_{P-C} = 39 Hz), 237.2 (s, 1C), 199.2 (s, 2C), 195.5 (s, 1C), 192.9 (s, 2C), 192.4 (s, 2C). ³¹P NMR (CD₂Cl₂, RT): δ 367.1 (s). Elemental analysis: Found: C, 38.18; H, 2.80. C₃₂H₂₇O₁₀PMoRu₃ calcd.: C, 38.37; H, 2.72%.

Spectral data of 6: MS (FAB, ⁹⁸Mo, ¹⁰²Ru), *m/z* 928 (M⁺); IR (C₆H₁₂)ν(CO): 2063s, 2026vs, 2000vw, 1991m, 1973s, 1962m, 1893w, 1870m, 1796m cm⁻¹; ¹H NMR (CDCl₃, RT): δ 8.19–8.11 (m, 2H), 7.66 (m, 3H), 1.80 (s, 15H), -19.14 (d, J_{P-H} = 11.2 Hz). ¹³C NMR (CDCl₃, RT): CO, δ 261.7 (s, 1C), 245.0 (d, 1C, J_{P-C} = 30 Hz), 222.5 (d, 1C, J_{P-C} = 14 Hz), 198.5 (s, 1C), 197.6 (d, 3C, J_{P-C} = 8 Hz), 195.7 (s, 1C), 192.2 (s, 1C), 191.9 (s, 1C). ³¹P NMR (CDCl₃, RT): δ 410.7 (s). Elemental analysis. Found: C, 32.25; H, 2.32. C₂₇H₂₃-Cl₂O₁₀PMoRu₃ calcd.: C, 32.16; H, 2.30%.

Spectral data of 7: MS (FAB, ⁹⁸Mo, ¹⁰²Ru), *m/z* 770 (M⁺); IR (C₆H₁₂) ν(CO): 2082s, 2061vs, 2021vs, 1995m, 1867w, br, 1819w, br cm⁻¹; ¹H NMR (CDCl₃, RT): δ 7.88 (m, 2H), 7.64 (m, 3H), 1.84 (s, 15H), -19.04 (d, 1H, J_{P-H} = 14.3 Hz). ¹³C NMR (CD₂Cl₂, 213 K): CO, δ 239.9 (s, 2C), 197.3 (d, 2C, J_{P-C} = 43 Hz), 192.3 (d, 2C, J_{P-C} = 7 Hz), 192.1 (d, 2C, J_{P-C} = 4 Hz); δ 135.9 (d, 1C, J_{P-C}) = 14 Hz, 135.2 (d, 2C), J_{P-C} = 11 Hz), 131.1 (d, 1C, J_{P-C} = 4 Hz), 129.4 (d, 2C, J_{P-C} = 11 Hz). ³¹P NMR (CDCl₃, RT): δ 299.9 (s). Elemental analysis. Found: C, 37.60; H, 2.89. C₂₄H₂₁O₈PMoRu₂ calcd.: C, 37.61; H, 2.76%.

2.2.1. Thermolysis of 5

A toluene solution (30 ml) of 5 (50 mg, 0.050 mmol) was heated to reflux for 20 min, during which the colour changed from dark-brown to red. The solvent was evaporated and the residue separated by thin layer chromatography (dichloromethane:hexane = 1 : 1) to afford 25 mg of 6 (0.027 mmol, 54%) as red-orange powder.

2.2.2. Reaction of 6 with carbon monoxide

A toluene solution (30 ml) of 6 (60 mg, 0.065 mmol) was refluxed under 1 atm of carbon monoxide for 15 min, during which the colour changed from red to orange. The solvent was evaporated and the residue was separated by thin layer chromatography (dichloromethane:hexane = 1 : 7), giving 3 mg of Ru₃(CO)₁₂

(0.012 mmol) and 37 mg of **7** (0.049 mmol, 75%) as orange powder.

2.2.3. Thermolysis of **7**

A toluene solution (30 ml) of **7** (100 mg, 0.099 mmol) was heated to reflux for two hours, during which the colour changed from orange-red to dark-brown. After allowing the solution to cool to room temperature, the solvent was evaporated and the residue was separated by thin layer chromatography (dichloromethane:hexane = 1:1), giving 20 mg of orange-red **7** (0.026 mmol), 4 mg of red **6** (0.004 mmol, 3%) and 45 mg of dark-brown Cp*Mo₂Ru₄(CO)₁₂(μ-PPh)₂ (**8**, 0.032 mmol, 49%). Crystals of **8** suitable for X-ray analysis were obtained by recrystallization from a layered solution of dichloromethane-methanol at room temperature.

Spectral data of **8**: MS (FAB, ⁹⁸Mo, ¹⁰²Ru), *m/z* 1426 (M⁺); IR (C₆H₁₂) ν(CO): 2051vs, 2019m, 1996s, 1974w, 1960m, 1944w, 1933w, 1917w, 1863vw, br, 1791w, br cm⁻¹; ¹H NMR (CDCl₃, RT): δ 7.77–7.01 (m, 10H), 1.88 (s, 15H), 1.65 (s, 15H). ¹³C NMR (CDCl₃, 218 K): CO, δ 271.5 (d, *J*_{P-H} = 8.5 Hz), 256.0 (d, *J*_{P-H} = 8 Hz), 235.2 (d, *J*_{P-H} = 8 Hz), 231.0, 217.9, 211.8, 203.8 (dd, *J*_{P-H} = 33 and 9.7 Hz), 200.5, 200.3 (d, *J*_{P-H} = 29.6 Hz), 193.4, 190.6, 184.3. ³¹P NMR (CDCl₃, RT): δ 463.8 (s), 382.5 (s). Elemental analysis. Found: C, 36.17; H, 2.98. C₄₅H₄₂Cl₂O₁₂P₂Mo₂Ru₄ calcd.: C, 35.94; H, 2.82%.

2.3. X-ray crystallography

Lattice parameters of **5** were determined from 25 randomly selected high angle reflections with 2θ angles in the range 19.00–25.00. The space group *P* 2₁ was identified on the basis of systematic absences and intensity statistics. All reflections were corrected for Lorentz, polarization and absorption effects. The absorption corrections were made by the Ψ scan method and the minimum and maximum transmission factors were 0.796 and 1.000, respectively. All data reduction and refinement were performed using the NRCC-SDP-VAX packages. The structures were solved by direct method and refined by least squares cycle; all non-hydrogen atoms were refined with anisotropic thermal parameters. The position of the bridging hydride ligands was obtained from a difference Fourier synthesis and refined accordingly. The hydrogen atoms of the phenyl and pentamethylcyclopentadienyl groups were calculated in the idealized positions with a fixed temperature coefficient (*U*_H = *U*_C + 0.01 Å²) and included in the structure factor calculation.

Lattice parameters of **8** were determined from 25 randomly selected high angle reflections with 2θ angles in the range 18.64–25.26; the space group *C*2/*c* was identified from the systematic absences and centric intensity distribution of the data, and confirmed by

successfully solving the crystal structure. The absorption corrections were made by Ψ scan method and the minimum and maximum transmission factors are 0.925 and 1.000, respectively. All data reduction and refinement were performed using the NRCC-SDP-VAX packages. In the final stage of refinement, a CH₂Cl₂ molecule that came from the solvent mixture of recryst-

TABLE 2. Atomic coordinates and equivalent isotropic displacement coefficients for **5**

	<i>x</i>	<i>y</i>	<i>z</i>	<i>B</i> _{iso}
Mo	-0.28078(5)	-0.54439(6)	-0.20248(3)	2.333(21)
Ru1	-0.37158(5)	-0.78091	-0.13232(3)	2.467(20)
Ru2	-0.42350(5)	-0.72791(5)	-0.31728(3)	2.329(20)
Ru3	-0.54922(4)	-0.58321(5)	-0.19797(3)	2.213(20)
P	-0.64113(15)	-0.72150(18)	-0.30693(10)	2.63(7)
O1	-0.3382(5)	-0.7601(5)	0.0741(3)	6.3(3)
O2	-0.1441(4)	-0.9475(5)	-0.1312(4)	6.3(3)
O3	-0.5219(4)	-1.0181(4)	-0.1370(3)	3.93(23)
O4	-0.4066(5)	-1.0045(4)	-0.3411(3)	5.7(3)
O5	-0.4182(5)	-0.6621(6)	-0.5143(3)	6.1(3)
O6	-0.6716(5)	-0.3510(5)	-0.2806(3)	5.8(3)
O7	-0.7079(4)	-0.5632(5)	-0.0468(3)	4.58(25)
O8	-0.1367(4)	-0.7621(5)	-0.2982(3)	4.29(25)
O9	-0.3921(4)	-0.4377(5)	-0.0353(3)	4.6(3)
O10	-0.0944(5)	-0.6513(5)	-0.0459(4)	6.9(3)
C1	-0.3514(6)	-0.7645(6)	-0.0036(4)	3.5(3)
C2	-0.2242(6)	-0.8814(7)	-0.1327(4)	3.9(3)
C3	-0.4710(6)	-0.9281(6)	-0.1376(4)	2.9(3)
C4	-0.4127(6)	-0.9014(7)	-0.3327(4)	3.7(3)
C5	-0.4261(6)	-0.6841(6)	-0.4396(4)	3.4(3)
C6	-0.6240(6)	-0.4391(7)	-0.2506(4)	3.4(3)
C7	-0.6490(5)	-0.5705(6)	-0.1055(4)	2.9(3)
C8	-0.2336(6)	-0.7191(7)	-0.2871(4)	3.7(3)
C9	-0.3823(6)	-0.4906(6)	-0.1022(4)	3.6(3)
C10	-0.1721(6)	-0.6247(7)	-0.1043(4)	4.1(3)
C11	-0.7211(5)	-0.8600(6)	-0.2759(4)	2.9(3)
C12	-0.7856(6)	-0.8636(7)	-0.2008(5)	4.0(4)
C13	-0.8436(7)	-0.9702(9)	-0.1799(5)	5.9(5)
C14	-0.8391(7)	-1.0737(8)	-0.2309(5)	5.6(4)
C15	-0.7783(6)	-1.0705(7)	-0.3062(5)	4.8(4)
C16	-0.7205(6)	-0.9650(7)	-0.3288(4)	3.7(3)
C17	-0.7492(6)	-0.6634(6)	-0.4038(4)	2.9(3)
C18	-0.8615(6)	-0.7208(7)	-0.4370(4)	3.9(3)
C19	-0.9358(7)	-0.6731(8)	-0.5128(5)	5.3(4)
C20	-0.9036(7)	-0.5685(9)	-0.5536(4)	5.7(4)
C21	-0.7967(7)	-0.5089(9)	-0.5199(4)	5.6(5)
C22	-0.7186(6)	-0.5580(7)	-0.4469(4)	4.1(4)
C23	-0.1684(6)	-0.4514(6)	-0.3112(4)	3.3(3)
C24	-0.2735(6)	-0.3770(6)	-0.3026(4)	3.3(3)
C25	-0.2615(6)	-0.3310(6)	-0.2125(4)	3.2(3)
C26	-0.1475(7)	-0.3817(7)	-0.1650(5)	4.4(4)
C27	-0.0914(6)	-0.4560(7)	-0.2276(5)	3.9(3)
C28	-0.1381(7)	-0.5035(8)	-0.3989(5)	5.6(5)
C29	-0.3703(7)	-0.3359(7)	-0.3781(5)	4.5(4)
C30	-0.3397(8)	-0.2307(7)	-0.1790(5)	5.5(4)
C31	-0.0921(9)	-0.3426(8)	-0.0714(5)	7.3(5)
C32	0.0382(6)	-0.5120(9)	-0.2083(6)	7.4(5)
H1	-0.453(4)	-0.574(5)	-0.293(3)	4.1(13)
H2	-0.506(4)	-0.725(5)	-0.127(3)	4.1(11)

tallization was located on the difference Fourier map; the carbon and chlorine atoms were then included in the analysis and refined accordingly. The combined

TABLE 3. Atomic coordinates and equivalent isotropic displacement coefficients for 8

	<i>x</i>	<i>y</i>	<i>z</i>	<i>B</i> _{iso}
Ru1	0.127167(12)	0.04337(6)	0.182141(24)	2.244(23)
Ru2	0.104508(12)	-0.19708(6)	0.215971(24)	2.436(25)
Ru3	0.133568(12)	-0.05405(6)	0.313322(23)	2.69(3)
Ru4	0.182483(12)	-0.01673(6)	0.246046(23)	2.232(24)
Mo1	0.157945(12)	-0.19053(6)	0.143955(24)	2.085(25)
Mo2	0.066946(13)	-0.03662(8)	0.13343(3)	3.29(3)
P1	0.15510(4)	-0.22254(19)	0.25071(8)	2.36(8)
P2	0.17303(4)	0.02659(18)	0.14520(7)	2.33(8)
O1	0.12348(12)	0.2881(5)	0.25969(23)	5.1(3)
O2	0.11142(12)	0.2384(6)	0.0835(3)	6.5(3)
O3	0.09684(9)	-0.1411(5)	0.07886(18)	2.91(22)
O4	0.08933(12)	-0.4815(5)	0.19665(25)	5.8(3)
O5	0.06688(10)	-0.1881(6)	0.32475(21)	5.8(3)
O6	0.03618(11)	-0.2595(7)	0.1986(3)	7.4(4)
O7	0.09399(12)	0.1442(6)	0.37120(23)	6.3(3)
O8	0.12962(12)	-0.2180(6)	0.42632(21)	5.8(3)
O9	0.18682(12)	0.0552(7)	0.38527(22)	7.1(4)
O10	0.24514(10)	-0.1095(6)	0.26429(25)	5.5(3)
O11	0.20111(12)	0.2665(5)	0.26789(24)	5.4(3)
O12	0.05721(11)	0.1282(6)	0.25009(24)	6.2(3)
C1	0.12491(15)	0.1912(7)	0.2332(3)	3.5(3)
C2	0.11462(15)	0.1538(7)	0.1173(3)	3.7(4)
C3	0.11716(14)	-0.1485(7)	0.1213(3)	2.5(3)
C4	0.09538(15)	-0.3758(8)	0.2027(3)	3.8(4)
C5	0.08401(14)	-0.1804(8)	0.2889(3)	3.6(4)
C6	0.05367(15)	-0.1889(8)	0.1797(3)	4.5(4)
C7	0.10853(15)	0.0702(8)	0.3477(3)	3.7(4)
C8	0.13113(15)	-0.1550(8)	0.3835(3)	3.7(4)
C9	0.17125(16)	0.0190(8)	0.3435(3)	4.5(4)
C10	0.22085(14)	-0.0760(7)	0.2578(3)	3.2(3)
C11	0.19452(15)	0.1607(7)	0.2598(3)	3.3(3)
C12	0.06314(15)	0.0661(8)	0.2093(3)	3.9(4)
C13	0.16831(14)	-0.3574(7)	0.3006(3)	2.7(3)
C14	0.14862(15)	-0.4440(8)	0.3234(3)	3.9(4)
C15	0.15809(17)	-0.5407(8)	0.3644(3)	5.1(4)
C16	0.18709(17)	-0.5515(8)	0.3822(3)	4.3(4)
C17	0.20665(16)	-0.4683(8)	0.3608(3)	4.5(4)
C18	0.19777(15)	-0.3724(7)	0.3184(3)	3.9(4)
C19	0.19223(14)	0.1428(7)	0.0993(3)	2.6(3)
C20	0.21908(14)	0.1958(7)	0.1197(3)	3.1(3)
C21	0.23286(15)	0.2875(8)	0.0855(3)	4.3(4)
C22	0.21980(18)	0.3294(8)	0.0318(3)	4.9(4)
C23	0.19288(18)	0.2788(9)	0.0106(3)	5.1(4)
C24	0.17899(15)	0.1850(7)	0.0440(3)	3.7(4)
C25	0.14994(15)	-0.3623(7)	0.0743(3)	3.0(3)
C26	0.17150(16)	-0.4060(7)	0.1204(3)	3.4(3)
C27	0.19682(14)	-0.3273(7)	0.1171(3)	3.2(3)
C28	0.19141(14)	-0.2351(7)	0.0690(3)	3.2(3)
C29	0.16224(15)	-0.2563(7)	0.0432(3)	3.1(3)
C30	0.12191(17)	-0.4309(8)	0.0555(3)	5.0(4)
C31	0.16805(20)	-0.5245(8)	0.1573(3)	5.5(5)
C32	0.22558(17)	-0.3489(9)	0.1514(3)	5.3(5)
C33	0.21453(17)	-0.1486(8)	0.0439(4)	5.3(5)
C34	0.14785(17)	-0.1867(8)	-0.0113(3)	4.4(4)

TABLE 3 (continued)

	<i>x</i>	<i>y</i>	<i>z</i>	<i>B</i> _{iso}
C35	0.03824(17)	0.1323(9)	0.0883(4)	5.9(5)
C36	0.01905(16)	0.0330(11)	0.1176(3)	6.6(5)
C37	0.02073(17)	-0.0819(12)	0.0838(4)	8.5(6)
C38	0.03835(17)	-0.0688(10)	0.0402(3)	6.5(5)
C39	0.05014(15)	0.0565(9)	0.0398(3)	4.4(4)
C40	0.0391(3)	0.2684(12)	0.0985(6)	16.1(10)
C41	-0.00280(21)	0.0512(19)	0.1618(4)	17.4(13)
C42	0.00060(24)	-0.2037(14)	0.0909(5)	12.2(9)
C43	0.04464(24)	-0.1782(13)	-0.0058(5)	11.0(8)
C44	0.06894(20)	0.0974(13)	-0.0093(4)	9.7(8)
C45	0.4397(3)	-0.0640(15)	0.1548(8)	21.4(14)
Cl1	0.47519(18)	-0.0308(9)	0.1778(4)	40.5(11)
Cl2	0.4399(3)	0.0021(8)	0.0894(4)	56.4(15)

TABLE 4. Selected bond distances (Å) and bond angles (°) for 5 (esd's in parentheses)

Mo–Ru(1)	2.981(1)	Mo–Ru(2)	2.920(1)
Mo–Ru(3)	2.915(1)	Ru(1)–Ru(2)	2.795(1)
Ru(1)–Ru(3)	2.947(1)	Ru(2)–Ru(3)	2.840(1)
Ru(2)–P	2.357(2)	Ru(3)–P	2.329(2)
Mo–C(8)	2.367(7)	Ru(2)–C(8)	2.026(7)
Mo–C(9)	2.045(6)	Ru(3)–C(9)	2.358(7)
Mo–C(10)	1.949(6)	Ru(1)–C(1)	1.908(6)
Ru(1)–C(2)	1.919(7)	Ru(1)–C(3)	1.915(7)
Ru(2)–C(4)	1.901(7)	Ru(2)–C(5)	1.878(6)
Ru(3)–C(6)	1.880(7)	Ru(3)–C(7)	1.857(5)
Mo–H(1)	2.15(5)	Ru(2)–H(1)	1.75(6)
Ru(3)–H(1)	1.86(4)	Ru(1)–H(2)	1.58(4)
Ru(3)–H(2)	1.89(5)		
Mo–Ru(1)–C(1)	105.8(2)	Mo–Ru(1)–C(2)	100.5(2)
Ru(1)–Mo–C(10)	62.8(2)	Mo–Ru(2)–C(5)	109.5(2)
Mo–Ru(3)–C(6)	103.7(2)	Mo–C(8)O(8)	130.6(5)
Ru(2)–C(8)O(8)	146.4(6)	Mo–C(9)O(9)	151.7(5)
Ru(3)–C(9)O(9)	125.4(5)	Mo–C(10)O(10)	166.7(6)
Mean Ru–CO(terminal)	176.6(6)		

TABLE 5. Selected bond distances (Å) and bond angles (°) for 8 (esd's in parentheses)

Ru(1)–Ru(2)	2.776(1)	Ru(1)–Ru(3)	3.037(1)
Ru(1)–Ru(4)	2.856(1)	Ru(1)–Mo(1)	2.912(1)
Ru(1)–Mo(2)	2.978(1)	Ru(2)–Ru(3)	2.835(1)
Ru(2)–Mo(1)	2.979(1)	Ru(2)–Mo(2)	2.904(1)
Ru(3)–Ru(4)	2.770(1)	Ru(4)–Mo(1)	3.008(1)
Ru(1)–P(2)	2.287(2)	Ru(2)–P(1)	2.382(2)
Ru(3)–P(1)	2.441(2)	Ru(4)–P(1)	2.442(2)
Ru(4)–P(2)	2.266(2)	Mo(1)–P(1)	2.374(2)
Mo(1)–P(2)	2.314(2)	Mo(1)–C(3)	1.930(6)
Ru(1)–C(3)	2.393(6)	Ru(2)–C(3)	2.244(6)
Mo(2)–C(3)	2.575(6)	Mo(2)–O(3)	2.148(4)
C(3)–O(3)	1.267(7)	Mo(2)–C(6)	1.969(8)
Ru(2)–C(6)	2.389(7)	Ru(3)–C(9)	1.938(7)
Ru(4)–C(9)	2.257(7)	Mo(2)–C(12)	1.982(7)
Mo(1)–C(3)–O(3)	147.1(5)	Mo(2)–O(3)–C(3)	94.3(4)
Ru(1)–C(3)–Ru(2)	73.5(2)	Mo(2)–C(6)–O(6)	155.1(6)
Ru(3)–C(9)–O(9)	148.7(6)	Ru(4)–C(9)–O(9)	128.7(5)
Mo(2)–C(12)–O(12)	171.0(6)	Ru(2)–C(5)–O(5)	163.7(6)

data collection and refinement parameters are given in Table 1. Atomic positional parameters for **5** and **8** are presented in Tables 2 and 3, whereas data of selected bond angles and lengths are given in Tables 4 and 5, respectively. Tables of bond distances and angles, positional parameters of hydrogen atoms and anisotropic thermal parameters of nonhydrogen atoms and listings of the observed and calculated structural factors are available from YC.

3. Results and discussion

Treatment of triruthenium phosphido complex $\text{Ru}_3(\text{CO})_{10}(\mu\text{-H})(\mu\text{-PPh}_2)$ with excess $\text{Cp}^*\text{Mo}(\text{CO})_3\text{H}$ in refluxing toluene (20 min) produced the tetranuclear, black phosphido cluster $\text{Cp}^*\text{MoRu}_3(\text{CO})_{10}(\mu\text{-H})_2(\mu\text{-PPh}_2)$ in small amount (**5**, 4.7%), phosphinidene complex $\text{Cp}^*\text{MoRu}_3(\text{CO})_{10}(\mu_3\text{-H})(\mu_3\text{-PPh})$ (**6**, 13%) and trinuclear, orange phosphinidene cluster $\text{Cp}^*\text{MoRu}_2(\text{CO})_8(\mu\text{-H})(\mu_3\text{-PPh})$ (**7**, 43%), in addition to two homometallic phosphinidene complexes $\text{Ru}_4\text{-}$

$(\text{CO})_{13}(\mu_3\text{-PPh})$ and $\text{Ru}_5(\text{CO})_{15}(\mu_4\text{-PPh})$. The latter homometallic phosphinidenes are evidently produced by self-condensation of the precursor $\text{Ru}_3(\text{CO})_{10}(\mu\text{-H})(\mu\text{-PPh}_2)$; the tetraruthenium complex $\text{Ru}_4(\text{CO})_{13}(\mu_3\text{-PPh})$ was first prepared by Carty and coworkers via the thermal pyrolysis of $\text{Ru}_3(\text{CO})_9(\mu\text{-H})(\mu\text{-PPh}_2)$ in heptane solution [11], whereas the pentanuclear complex $\text{Ru}_5(\text{CO})_{15}(\mu_4\text{-PPh})$ was obtained from the reactions of $\text{Ru}_3(\text{CO})_{12}$ with $\text{CpMn}(\text{CO})_2(\text{PCl}_2\text{Ph})$ in small quantity [12] and the reaction with an equimolar amount of PPhH_2 in toluene [13].

3.1. Characterization of **5**

This complex shows a molecular ion in its FAB mass spectrum and fragmentation ions corresponding to successive loss of CO ligands. The solution IR spectrum exhibits seven terminal CO stretching absorptions and two additional weak absorptions at 1865 and 1805 cm^{-1} , indicating the presence of bridging CO ligands. The ^1H NMR spectrum shows two hydride signals at $\delta = 13.65$ (d, $J_{\text{P-H}} = 19.6$ Hz) and -19.52

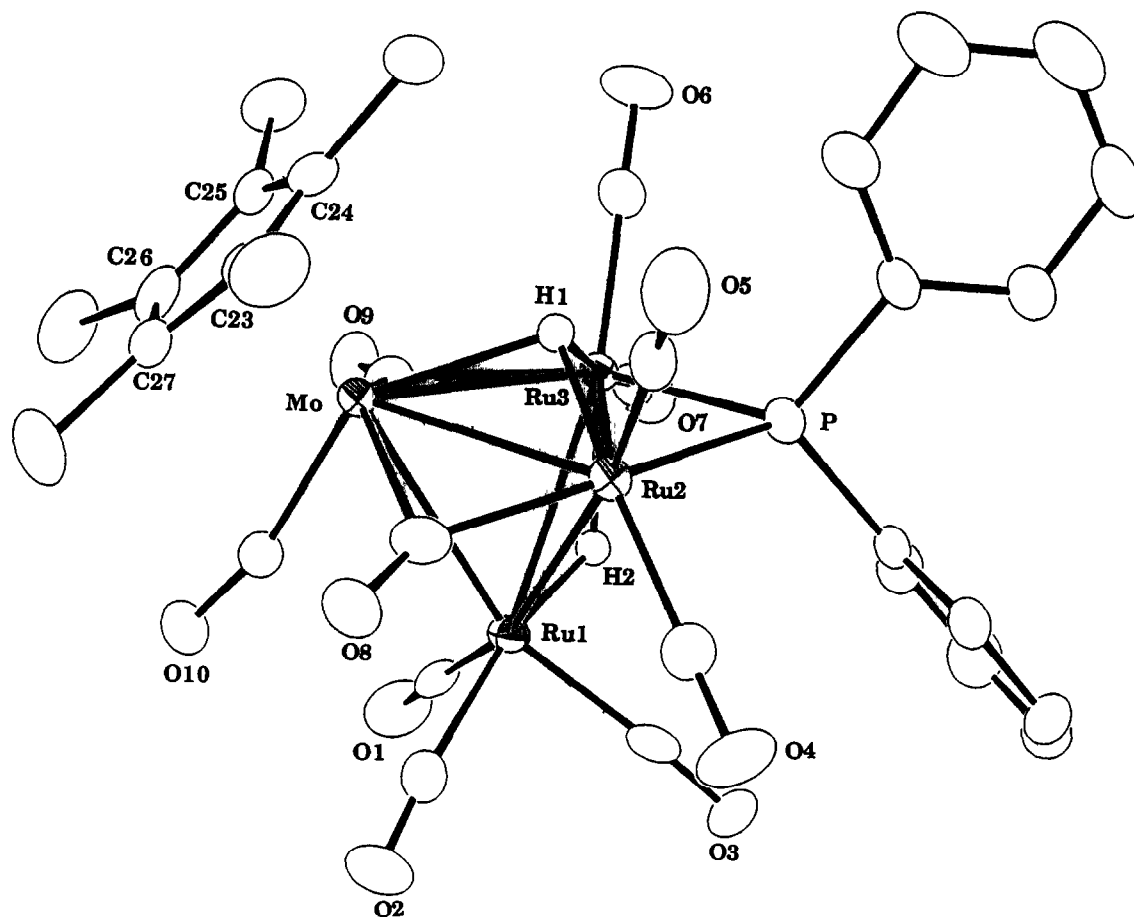


Fig. 1. Molecular structure of **5** and the atomic numbering scheme.

(d, $J_{P-H} = 11.2$ Hz) and several multiplets in the range δ 7.91–6.96, indicating the presence of two phenyl groups. The chemical shift value of signal at δ –19.52 is normal for an edge-bridging hydride and the downfield chemical shift for the hydride at δ –13.65 implies that it belongs to a rare, triply bridging hydride [14]. As these spectroscopic data do not uniquely define its molecular structure, a single-crystal X-ray analysis was carried out.

The molecular diagram is shown in Fig. 1, and selected bond parameters are presented in Table 3. The metal framework may be described as a distorted $MoRu_3$ tetrahedron, with metal–metal bond distances being in the range 2.795(1)–2.981(1) Å. The Ru(2)–Ru(3) edge (2.840(1) Å), which is bridged by the phosphido ligand, is intermediate between the other two Ru–Ru bonds, Ru(1)–Ru(3) = 2.947(1) and Ru(1)–Ru(2) = 2.795(1) Å. The Ru(2)–P and Ru(3)–P distances of 2.357(2) and 2.329(2) Å, respectively, are in the range observed for previously reported ruthenium clusters containing phosphido ligands [15]. For example, in $Ru_4(\mu_4-C_2)(\mu-PPh_2)_2(CO)_{12}$, the corresponding value are 2.344(2) and 2.357(2) Å, respectively [15(b)]. In addition, there are eight terminal and two bridging CO ligands in the molecule. The bridging CO ligands lie on an extension of the metal triangle defined by the atoms Mo, Ru(2) and Ru(3). The three Ru atoms are each coordinated by three, two and two terminal CO ligands, respectively; the Mo atom is bonded to a Cp^* ligand and carries only one terminal CO ligand.

The most striking aspect of the structure of **5** is the position of hydride ligands. Both hydride ligands have been unambiguously located in a difference Fourier synthesis; one occupies the Ru(1)–Ru(3) edge with Ru(1)–H(2) = 1.58(4) and Ru(3)–H(2) = 1.89(5) Å, and the second caps the $MoRu_2$ triangle, which is surrounded by two edge bridging CO and phosphido ligands, with the respective bond distances being Mo–H(1) = 2.15(5), Ru(2)–H(1) = 1.75(6) and Ru(3)–H(1) = 1.86(4) Å. The elongation of the Mo–H(1) bond may be ascribed to unfavourable steric interaction of the

Cp^* ligand with the Mo atom. The influence exerted on the Ru(1)–Ru(3) bond by the edge-bridging hydride H(2) is noticeable; it is considerably elongated (2.947(1) Å) relative to the Ru(1)–Ru(2) bond (2.795(1) Å) that possesses no bridging hydride. The coordination behaviour of the face-bridging hydride is comparable to that of the tetranuclear cluster complexes $Fe_3Pt(CO)_{10}(\mu_3-H)(\mu_3-COMe)(PPh_3)$ [16] and $Co_3Fe(CO)_9(\mu_3-H)(P(OMe)_3)_3$ [17]. A few face-bridging hydrides have also been observed for trinuclear cluster and higher nuclearity clusters.

The fluxionality of the bridging hydrides has been revealed by ^{13}C NMR study. In contrast to the crystal structure which possesses no apparent symmetry, the ^{13}C NMR spectrum recorded at room temperature shows only six CO signals at δ 242.5 ($J_{P-C} = 39$ Hz), 237.2, 199.2, 195.5, 192.9 and 192.4 in the ratio 2:1:2:1:2:2 (Fig. 2). The doublet at δ 242.5 is due to the unique bridging CO ligands, because of its downfield chemical shift and large $^2J_{P-C}$ coupling with the phosphorus atom which is located at the *trans* position. The signals at δ 237.2 and 195.5 are assigned to the Mo–CO and the axial CO on atom Ru(1), respectively. On the basis of these spectral assignments, we deduce that the edge-bridging hydride ligand undergoes rapid migration between the Ru(1)–Ru(3) and Ru(1)–Ru(2) bonds, which generates a time-averaged mirror plane and simplifies the pattern of CO resonances but fails to average the local environment of hydrides in the 1H NMR spectrum at the same temperature. However, irradiation of either hydride signal under the conditions of a NMR spin-saturation transfer experiment suppressed the second hydride signal, suggesting that exchange between edge and triply bridging hydride is feasible at this temperature, but the energy barrier is slightly greater than that for the migration of the edge-bridging hydride ligand. A similar hydride migration between the adjacent Ru–Ru bonds was established for the heterometallic cluster $CpWRu_3(CO)_{11}(\mu-H)_2(AuPPh_3)$ [18], for which exchange between edge- and face-bridging was not detected at temperature below 240 K.

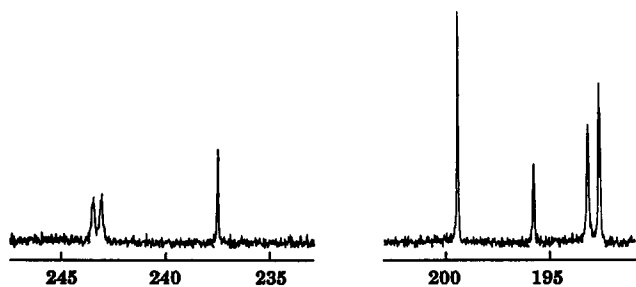


Fig. 2. ^{13}C -(1H) NMR spectrum (100.6 MHz) of **5** recorded at 294 K, showing the region of CO resonances.

3.2. Characterization of 6 and 7

Complexes 6 and 7 were characterized by spectral methods. The ^{13}C NMR spectrum of 6 shows two bridging CO resonances at δ 261.7 and 245.0 ($J_{\text{P-C}} = 30$ Hz), a Mo-CO resonance at δ 222.5 ($J_{\text{P-C}} = 14$ Hz) and five Ru-CO resonances in the range δ 198.5–191.9 in the ratio 1:3:1:1:1. The ^1H NMR spectrum which reveals a signal at δ -19.14 for the hydride, and ^{31}P NMR spectrum which exhibits a phosphinidene signal at δ 410.7, which is near the value found for μ_3 -phosphinidene ligands in Ru_4 clusters [19], supplement the information obtained from the ^{13}C NMR spectrum. In addition, the $\nu(\text{CO})$ pattern in solution IR spectrum, featuring seven terminal CO bands in the range 2063–1893 cm^{-1} and two bridging CO stretching bands at 1870 and 1796 cm^{-1} , is fully comparable with that of a structurally characterized WRu_3 analogue 2. These experimental data provide unambiguous proof of the proposed structure.

Likewise, the ^1H and ^{31}P NMR spectra of 7 exhibit a hydride signal at δ -19.04 ($J_{\text{P-H}} = 14.3$ Hz) and a

phosphinidene resonance at δ 299.9, respectively; no observation of a second set of hydride and phosphinidene signals was made even at 200 K, suggesting that this molecule contains only one isomer in solution. The ^{13}C NMR spectrum recorded at 213 K, showing four CO signals at δ 239.9, 197.3 ($J_{\text{P-C}} = 43$ Hz), 192.3 ($J_{\text{P-C}} = 7$ Hz) and 192.1 ($J_{\text{P-C}} = 4$ Hz) in an intensity ratio 2:2:2:2, implies that the hydride is located on the unique Ru-Ru edge in solution. As verified by this low-temperature ^{13}C NMR work, complex 7 in solution is isostructural with the phosphinidene cluster 1a and the imido clusters $\text{LWRu}_2(\text{CO})_8(\mu\text{-H})(\mu_3\text{-NPh})$. In contrast, a solution of the Cp^*WRu_2 analogue 1b contains two interconvertible isomers, which are related by rapid hydride migration between W-Ru and Ru-Ru edges.

3.3. Characterization of 8

Thermolysis of 7 in refluxing toluene solution induced elimination of H_2 and caused dimerization to afford hexanuclear 8 in 49% yield. The ^{13}C NMR

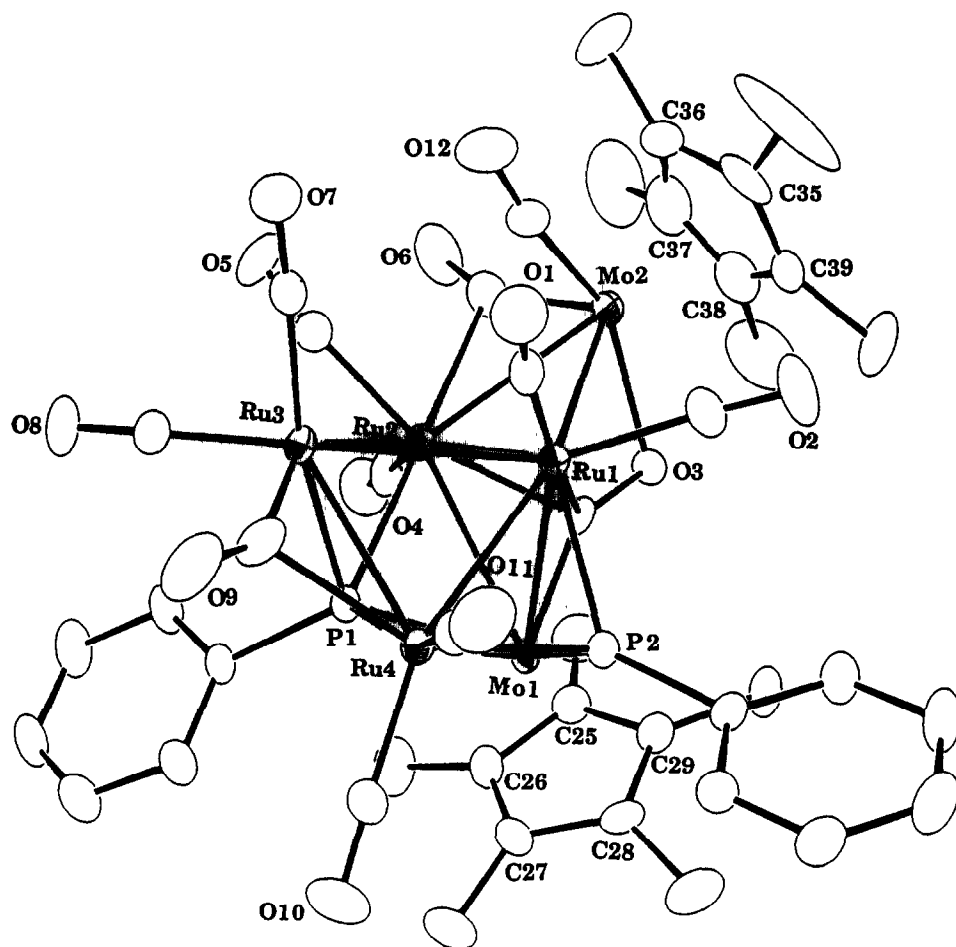


Fig. 3. Molecular structure of 8 and the atomic numbering scheme.

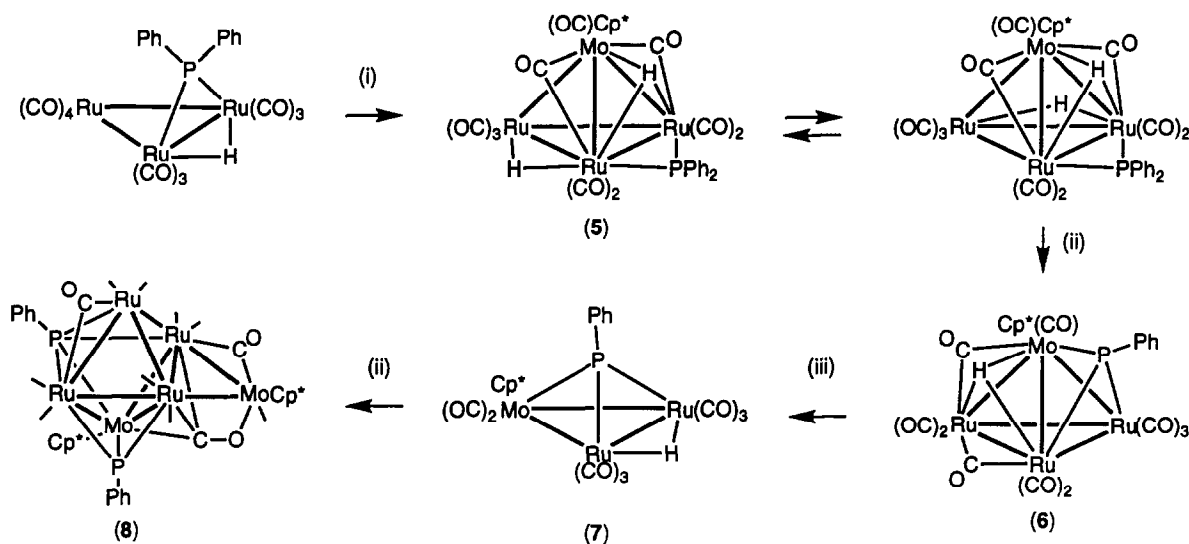
spectrum recorded at 218 K shows an η^2 -CO signal at δ 271.5 ($J_{\text{P-H}} = 8.5$ Hz), the bridging Mo(μ -CO)Ru signal at δ 256.0 ($J_{\text{P-H}} = 8$ Hz), the bridging Ru(μ -CO)Ru signal at δ 235.2 ($J_{\text{P-H}} = 8$ Hz), the terminal Mo-CO signal at δ 231.0 and eight terminal Ru-CO resonances in the range 217.9–184.3. The low temperature ^{13}C NMR data of the W_2Ru_4 analogue **4** reported earlier assists the assignment.

The crystal structure of **8** was also determined by single-crystal X-ray diffraction. A molecular drawing appears in Fig. 3 while the essential bond distances and angles are summarized in Table 5. Compound **8** possesses a hexanuclear core of two molybdenum and four ruthenium atoms coordinated by 12 CO ligands and two phosphinidene ligands. The core skeleton and ligand arrangement is virtually the same as that of the related W_2Ru_4 cluster **4**, comprising an edge-bridged square pyramidal MoRu_4 central core, a tentacle Mo metal unit, two phosphinidene ligands, and a μ_4 - η^2 -CO ligand encapsulated in the cavity of the Mo_2Ru_2 butterfly. In this molecule all metal-metal bonds are normal with Ru-Ru distances in the range 2.770(1)–3.037(1) Å and Mo-Ru distances in the narrow range 2.904(1)–3.006(1) Å; one μ_3 -phosphinidene ligand occupies a MoRu_2 metal triangle and a second μ_4 -phosphinidene takes the MoRu_3 square face. If we consider that the μ_4 -phosphinidene ligands are part of the cluster core, the molecule appears to adopt a MoRu_4P octahedral core bridged by a μ_3 -phosphinidene and a $\text{Cp}^*\text{Mo}(\text{CO})_2$ fragment. A few cluster complexes containing both μ_4 - and μ_3 -phosphinidene ligands [20] or clusters with the unique μ_4 - η^2 -CO ligand [21] have been documented.

4. Summary

Reactions performed in this work are summarized in Scheme 2. Condensation of $\text{Ru}_3(\text{CO})_{10}(\mu\text{-H})(\mu\text{-PPh}_2)$ and $\text{Cp}^*\text{Mo}(\text{CO})_3\text{H}$ proved to be a convenient method to generate the MoRu_3 phosphido cluster **5**. Its formation is best interpreted as a cluster condensation, in which the reaction proceeded via formation of unsaturated $\text{Ru}_3(\text{CO})_9(\mu\text{-H})(\mu\text{-PPh}_2)$, followed by addition of one molecule of $\text{Cp}^*\text{Mo}(\text{CO})_3\text{H}$. Thermolysis of **5** in toluene produced the phosphinidene cluster **6** in moderate yield via elimination of a benzene molecule. Isolation of **5** provides unambiguous evidence that, for the MoRu_3 phosphinidene cluster **6**, the formation of tetrahedral cluster core occurred prior to the generation of phosphinidene ligand by elimination of benzene. In contrast, Mays and coworkers reported that the tetrahedral phosphinidene cluster complexes can be prepared by condensation of anionic phosphinidene cluster $[\text{Ru}_3(\text{CO})_9(\mu\text{-H})(\mu_3\text{-PPh})]^-$ with a cationic, mononuclear metal fragment [22].

Furthermore, complex **6** reacted with CO to afford the trinuclear phosphinidene cluster **7** through cluster fragmentation. In contrast to the WRu_2 counterpart, it exists in solution as only one isomer, in which the hydride ligand is associated with the unique Ru-Ru edge [3]. The variation of isomer proportion indicates that molybdenum donates fewer electrons than tungsten, thus disfavoring the move of the hydride from the Ru-Ru to the Mo-Ru edge. Similar behaviour has also been noted upon replacing the Cp^* ligand with the less markedly electron-donating Cp ligand in the WRu_2 system [3]. When complex **7** was heated in



Scheme 2.

refluxing toluene, the hexanuclear cluster **8** was obtained. Interestingly, complex **8** remains the only Mo₂Ru₄ cluster observed in solution upon extending the reaction. This fruitless attempt indicates that the Mo₂Ru₄ analogue of hexanuclear W₂Ru₄ cluster **3** is probably absent. The factors controlling the geometry of the cluster skeleton remains a goal of further research.

Acknowledgment

We thank the National Science Council of the Republic of China for financial support (Grant No. NSC83-0208-M007-43).

References

- (a) D.A. Roberts and G.L. Geoffroy, in G. Wilkinson, F.G.A. Stone and E.W. Abel (eds.), *Comprehensive Organometallic Chemistry* Pergamon, Oxford, 1982, Vol. 6, Chapter 40; (b) D.F. Shriver, H.D. Kaesz and R.D. Adams (eds.), *The Chemistry of Metal Cluster Complexes*, VCH Publishers, New York, 1990.
- (a) Y. Chi, L.-K. Liu, G. Huttner and L. Zsolnai, *J. Organomet. Chem.*, **390** (1990) C50; (b) Y. Chi, H.-F. Hsu, L.-K. Liu, S.-M. Peng and G.-H. Lee, *Organometallics*, **11** (1992) 1763.
- R.-C. Lin, Y. Chi, S.-M. Peng and G.-H. Lee, *Inorg. Chem.*, **31** (1992) 3818.
- (a) Y. Chi, R.-C. Lin, S.-H. Peng and G.-H. Lee, *J. Cluster Sci.*, **3** (1992) 333; (b) R.-C. Lin, Y. Chi, S.-H. Peng and G.-H. Lee, *J. Chem. Soc., Dalton Trans.*, (1993) 227; (c) R.-C. Lin, Y. Chi, S.-H. Peng and G.-H. Lee, *J. Chem. Soc., Chem. Commun.*, (1992) 1705.
- J.-C. Wang, R.-C. Lin, Y. Chi, S.-H. Peng and G.-H. Lee, *Organometallics*, **12** (1993) 4061.
- C.E. Housecroft, in T.P. Fehlner (ed.), *Inorganometallic Chemistry*, Plenum Press, New York, 1992, Chapter 3.
- S.P. Rowley, P.S. White and C.K. Schauer, *Inorg. Chem.*, **31** (1992) 3158.
- M. Lanfranchi, A. Tiripicchio, E. Sappa and A.J. Carty, *J. Chem. Soc., Dalton Trans.*, (1986) 2737.
- D. Nucciarone, S.A. MacLaughlin and A.J. Carty, *Inorg. Synth.*, **26** (1989) 264.
- S.P. Nolan and C.D. Hoff, in R.B. King and J.J. Eisch (eds.), *Organometallic Syntheses*, Elsevier, New York, 1989, Vol. 4, p. 58.
- S.A. MacLaughlin, A.J. Carty and N.J. Taylor, *Can. J. Chem.*, **60** (1982) 87.
- K. Natarajan, L. Zsolnai and G. Huttner, *J. Organomet. Chem.*, **209** (1981) 85.
- J.S. Field, R.J. Haines and D.N. Smit, *J. Organomet. Chem.*, **224** (1982) C49.
- A.P. Humphries and H.D. Kaesz, *Prog. Inorg. Chem.*, **25** (1979) 146.
- (a) S.A. MacLaughlin, N.J. Taylor and A.J. Carty, *Organometallics*, **2** (1983) 1194; (b) M.I. Bruce, M.R. Snow, E.R.T. Tiekink and M.L. Williams, *J. Chem. Soc., Chem. Commun.*, (1986) 701; (c) M.I. Bruce, M.J. Liddell, B.W. Skelton and A.H. White, *Organometallics*, **10** (1991) 3282; (d) J.S. Field, R.J. Haines and F. Mulla, *J. Organomet. Chem.*, **439** (1992) C56.
- M. Green, K.A. Mead, R. Mills, I.D. Salter, F.G.A. Stone and P. Woodward, *J. Chem. Soc., Chem. Commun.*, (1982) 51.
- B.T. Huie, C.B. Knobler and H.D. Kaesz, *J. Am. Chem. Soc.*, **100** (1978) 3059.
- C.-C. Chen, Y. Chi, S.-H. Peng and G.-H. Lee, *J. Chem. Soc., Dalton Trans.*, (1993) 1823.
- F. Van Gastel, J.F. Corrigan, S. Doherty, N.J. Taylor and A.J. Carty, *Inorg. Chem.*, **31** (1992) 4492.
- (a) K. Kwek, N.J. Taylor and A.J. Carty, *J. Am. Chem. Soc.*, **106** (1984) 4636; (b) J.S. Field, R.J. Haines and F. Mulla, *J. Organomet. Chem.*, **389** (1990) 227.
- (a) M. Manassero, M. Sansoni and G. Longoni, *J. Chem. Soc., Chem. Commun.*, (1976) 919; (b) B.F.G. Johnson, J. Lewis, M. McPartlin, M. Pearsall and A. Sironi, *J. Chem. Soc., Chem. Commun.*, (1984) 1089; (c) C.P. Horwitz and D.F. Shriver, *Organometallics*, **3** (1984) 756; (d) C.P. Horwitz and D.F. Shriver, *J. Am. Chem. Soc.*, **107** (1985) 8147; (e) C.P. Horwitz, E.M. Holt, C.P. Brock and D.F. Shriver, *J. Am. Chem. Soc.*, **107** (1985) 8136; (f) R.D. Adams, J.E. Babin and M. Tasi, *Inorg. Chem.*, **27** (1988) 2618; (g) C.E. Anson, P.J. Bailey, G. Conole, B.F.G. Johnson, J. Lewis, M. McPartlin and H.R. Powell, *J. Chem. Soc., Chem. Commun.*, (1989) 442; (h) Y. Chi, F.-J. Wu, B.-J. Liu, C.-C. Wang and S.-L. Wang, *J. Chem. Soc., Chem. Commun.*, (1989) 873; (i) Y. Chi, S.-H. Chuang, L.-K. Liu and Y.-S. Wen, *Organometallics*, **10** (1991) 2485.
- M.J. Mays, P.R. Raithby, P.L. Taylor and K. Henrick, *J. Chem. Soc., Dalton Trans.*, (1984) 959.